Supplement of Hydrol. Earth Syst. Sci., 29, 4473–4489, 2025
https://doi.org/10.5194/hess-29-4473-2025-supplement

Hydrology and Earth System Sciences
Open Access
EGU

Supplement of

Imprints of increases in evapotranspiration on decreases in streamflow during dry periods, a large-sample analysis in Germany

Giulia Bruno et al.

Correspondence to: Giulia Bruno (giulia.bruno@slf.ch)

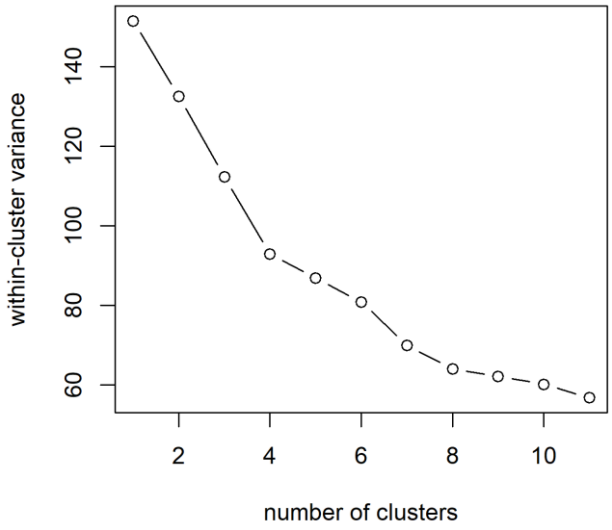

Fig. S1: Within-cluster variance for different numbers of clusters (Sect. 2.1).

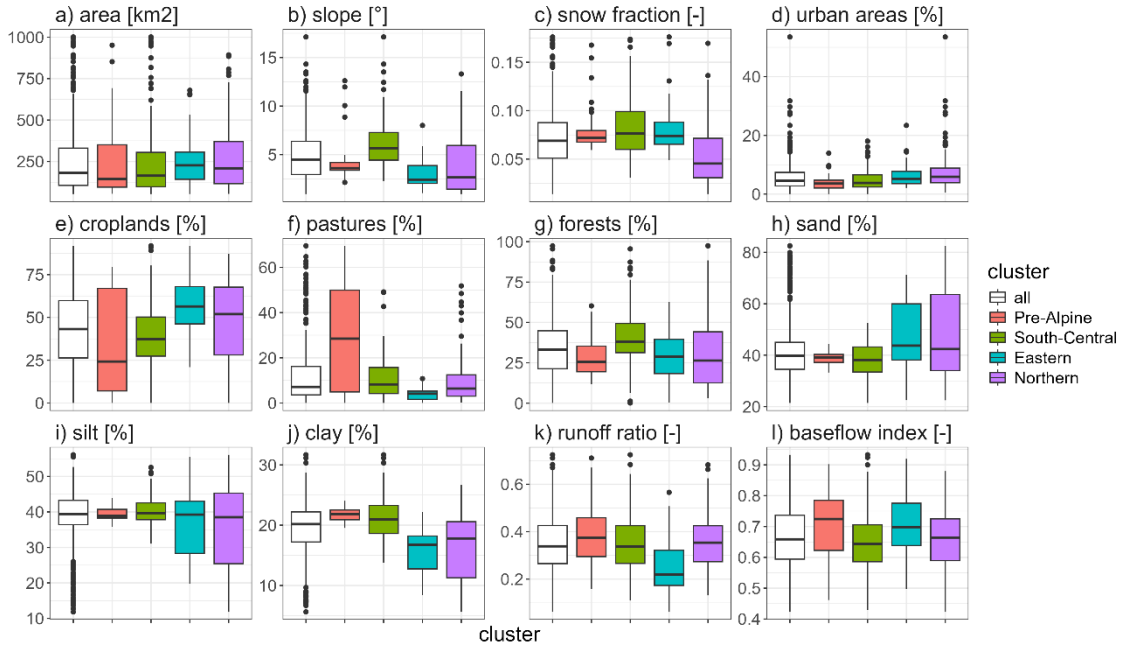

Fig. S2: Attributes of the study catchments. Boxplots of (a) area, (b) slope, (c) snow fraction, (d) urban, (e) cropland, (f) pastures, (g) forests, (h) sand, (i) silt, (j) clay, (k) runoff ratio, and (l) baseflow index for all catchments and by clusters. Details on the attributes are in Table 1.

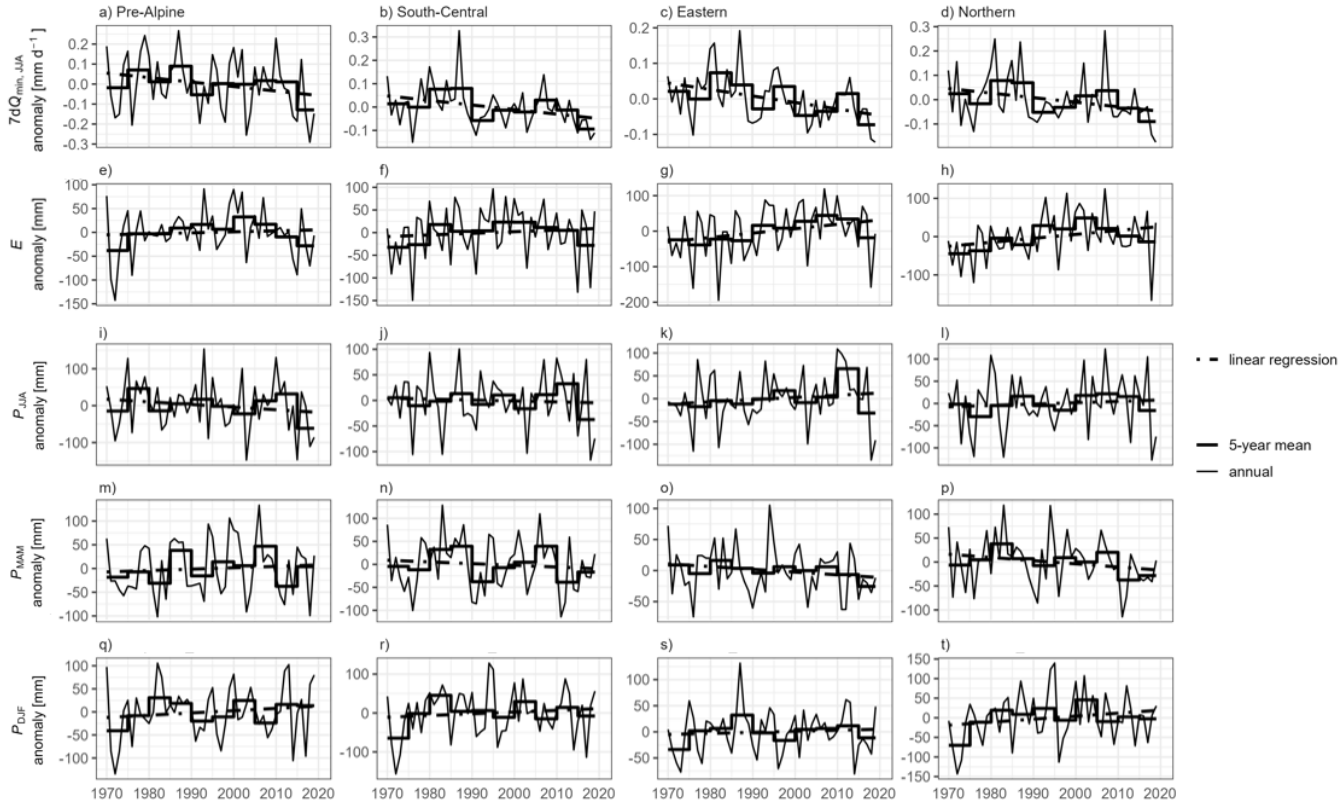

Fig. S3: Long-term variations in summer low flows ($7dQ_{min,\ JJA}$, panels a–d) and their potential predictors (annual evapotranspiration, E, e–h, precipitation over summer, P_{JJA}, i–l, spring, P_{MAM}, m–p, and winter P_{DJF}, q–t) over 1970–2019. Average anomalies across the catchments in each cluster.

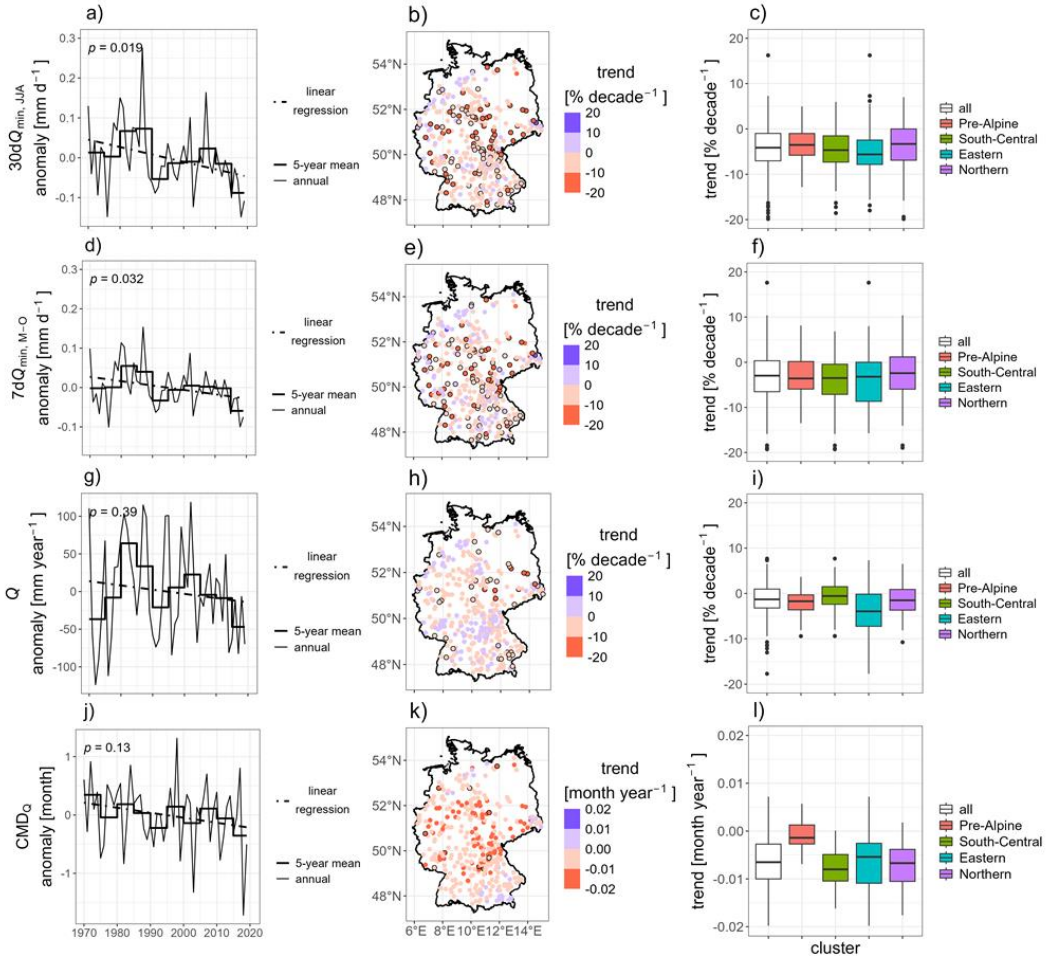

Fig. S4: Long-term variations in streamflow (*Q*) metrics over 1970–2019 (30d$Q_{min, JJA}$, panels a–c, and 7d$Q_{min, M-O}$, panels d–f, as metrics for summer low flows, annual *Q*, panels g–i, and the center of mass date of streamflow CMD_Q, panels j–l). (a, d, g, and j) Average anomalies across the study catchments. (b, e, h, and k) Map of catchment-scale trends (black edges if significant). (c, f, i, and l) Boxplots of trends for all catchments and by cluster.

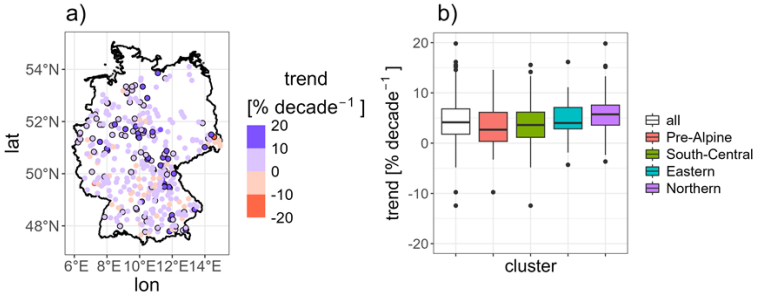

Fig. S5: Long-term variations annual catchment evapotranspiration (*E*) over 1970–1999. (a) Map of catchment-scale trends (black edges if significant). (b) Boxplots of trends for all catchments and by cluster.

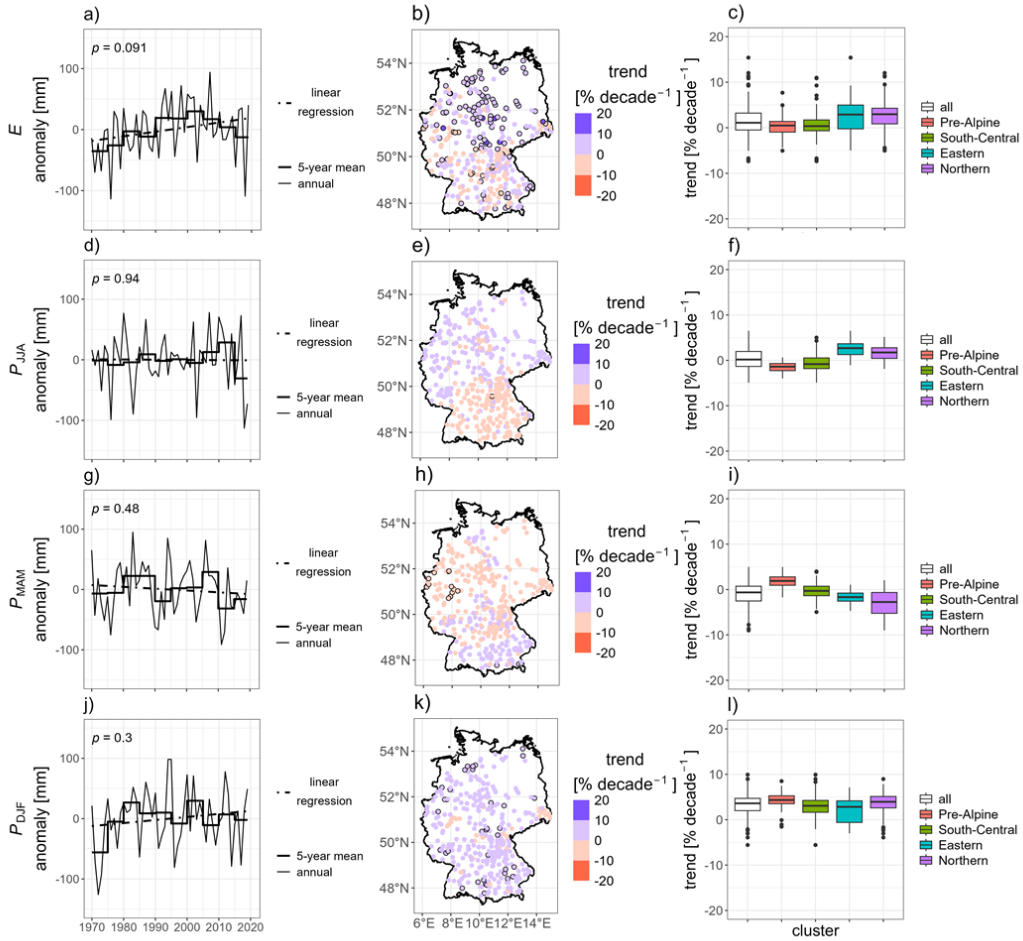

Fig. S6: Long-term variations in predictors of variations in summer low flows over 1970–2019 (annual evapotranspiration, *E*, panels a–c, precipitation over summer, P_{JJA}, panels d–f, spring, P_{MAM}, panels g–i, and winter P_{DJF}, panels j–l) from uncorrected precipitation for gauge undercatch (Sect. 2.2). (a, d, g, and j) Average anomalies across the catchments. (b, e, h, and k) Maps of catchment-scale trends (black edges if significant). (c, f, i, and l) Boxplots of trends for all catchments and by cluster.

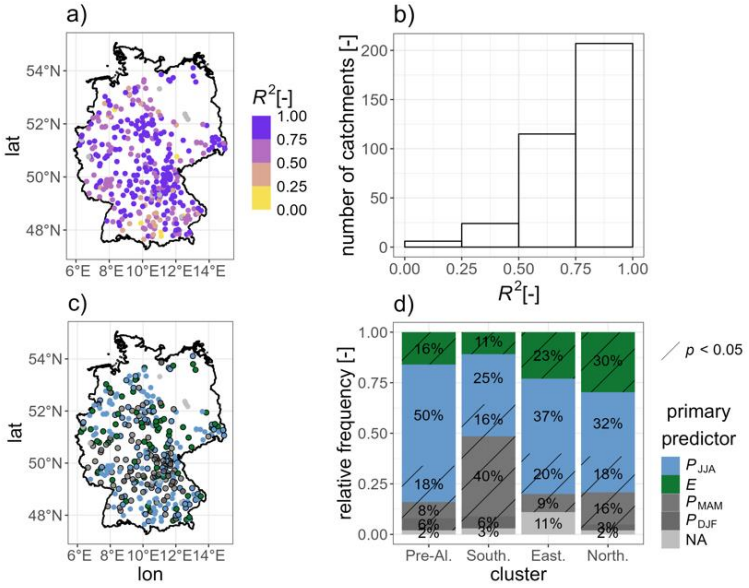

Fig. S7: Model results from the multiple linear regressions on catchment-scale data. (a) Map of coefficients of determination of the models (R^2). (b) Histogram of R^2. (c) Map of primary predictors (black edges if significant). (d) Relative frequency of primary predictors by cluster. Light grey in (a, c, and d) refers to catchments with high multicollinearity of the predictors, and thus excluded from the analysis (Sect. 2.5). In (d), Pre-al. refers to pre-Alpine, South. to south-central, East. to eastern, and North. to northern cluster.

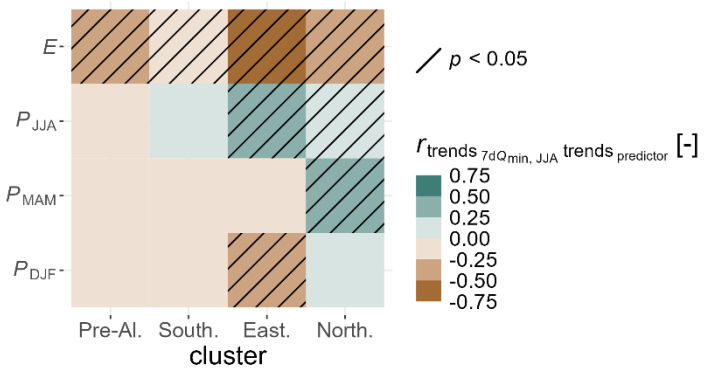

Fig. S8: Attribution of long-term variations in summer low flows to their predictors (strength of spatial coherence): Pearson's correlation coefficients (r) between catchment-scale trends in summer low flows ($7dQ_{min,\ JJA}$) and in potential predictors (annual evapotranspiration, E; summer precipitation, P_{JJA}; spring precipitation P_{MAM}; and winter precipitation, P_{DJF}) over 1970–1999, for the catchments in the different clusters. Pre-al. refers to pre-Alpine, South. to south-central, East. to eastern, and North. to northern cluster.

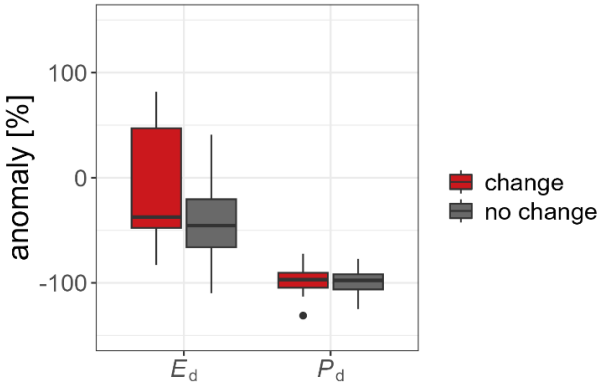

Fig. S9: Boxplots of mean anomalies over the multi-year drought between 1989 and 1993 in detrended annual evapotranspiration (E_d) and precipitation (P_d), for catchments with change and no change in the annual relationship between precipitation and streamflow during the multi-year drought.

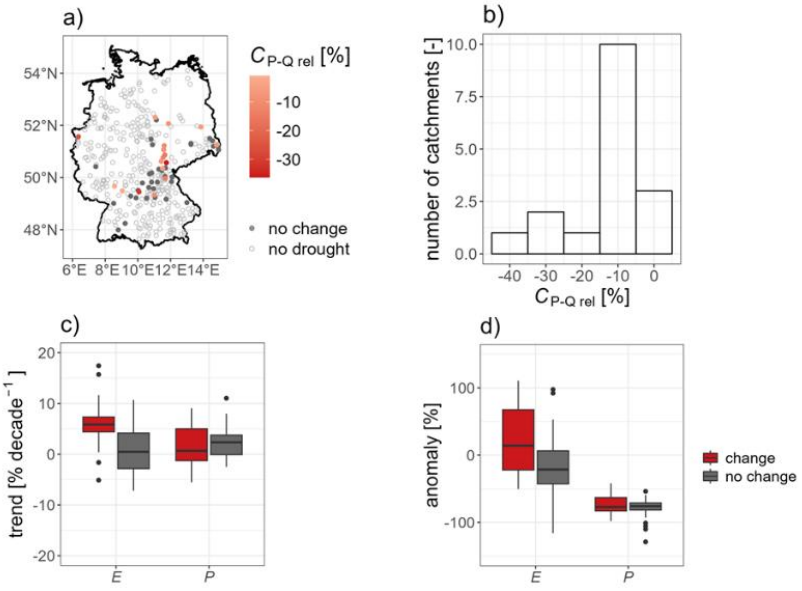

Fig. S10: Changes in the annual relationship between precipitation (*P*) and streamflow (*Q*, *P*-*Q* relationship) during the multi-year drought between 1989 and 1993, and their potential predictors, from uncorrected *P* for gauge undercatch (Sect. 2.2). (a) Map of the magnitude of changes in the *P*-*Q* relationship ($C_{P\text{-}Q\ rel}$), across the study catchments. (b) Histogram of $C_{P\text{-}Q\ rel}$. (c) Boxplots of trends in annual catchment actual evapotranspiration (*E*) and *P* over 1970–1993, for catchments with change and no change in the *P*-*Q* relationship. (d) Boxplots of mean anomalies in *E* and *P* over the drought, for catchments with change and no change in the *P*-*Q* relationship.

Table S1: Trends in summer low flows ($7dQ_{min,\ JJA}$) and their predictors (annual evapotranspiration, E, precipitation over summer, P_{JJA}, spring, P_{MAM}, and winter P_{DJF}) over 1970–2019.

Variable	Catchments with positive trends [%]	Catchments with negative trends [%]	Median trend across all catchments [% decade^{-1}]	Catchments with significant positive trends [%]	Median trend across catchments with significant positive trends [% decade^{-1}]	Catchments with significant negative trends [%]	Median trend across catchments with significant negative trends [% decade^{-1}]
$7dQ_{min,\ JJA}$	23	77	-3.7	2	7.4	31	-9.7
E	66	34	1.1	27	4.6	5	-4
P_{JJA}	52	48	0.2	0	-	0	-
P_{MAM}	34	66	-0.6	1	4.8	3	-6.9
P_{DJF}	90	10	3.6	10	6.9	0	-

Table S2: Model results from the multiple linear regressions on cluster-average data: coefficients of determination of the model (R^2) and standardized coefficients (Eq. 4, * if significant) for each cluster. α_1 refers to annual evapotranspiration, α_2 to summer precipitation (P), α_3 to spring P, and α_4 to winter P.

Cluster	R^2	α_1	α_2	α_3	α_4
Pre-Alpine	0.7	-0.16	0.89*	0.42	0.44
South-Central	0.87	-0.36	0.63*	0.76*	0.34
Eastern	0.95	-0.74*	0.64*	0.65*	0.09
Northern	0.94	-0.64*	0.67*	0.75*	0.25